

Performance of URM Wall with Opening Under In-plane Horizontal Loading



T.N. Chen , J.S. Chang & H.H. Huang

Department of Architecture, National Cheng Kung University, Tainan , Taiwan

SUMMARY:

The masonry wall is the most important element that provides earthquake resistance for the many historic buildings in Taiwan. The main purpose of this paper is to investigate the structural performance of URM wall with opening. In this study , five brick wall specimens were manufactured and tested under in-plane loading. The lime was added in the mortar to simulate the wall of historic building. From the test , it is observed that the main damage modes of the wall with opening includes the oblique crack in the diagonal corner area and the horizontal crack on the top and bottom of the piers between two openings. Base on the failure mode observed from the experiment , a procedure for evaluating the ultimate strength of URM wall with opening is developed in this study. The comparison shows the calculated resistant load has average difference less than 4% with the ultimate load act in experiment.

Keywords: Masonry, Brick wall, In-plane Loading, Historic building , Opening

1. INTRODUCTION

The wall element is the most important part that provides the earthquake resistance for most of the masonry historic buildings in Taiwan. The wall , due to the necessary of architectural function , usually has window or door openings. For this wall with opening. For masonry wall , so far numerous studies have been conducted. However , the studies related to the complete behaviour of URM wall with opening , especially the evaluation of ultimate strength is scarce. The main purpose of this paper is to investigate the behavior of URM wall with opening under horizontal load, and using the test results to develop a procedure for evaluating the ultimate strength of URM wall with opening.

2. EXPERIMENTAL SET-UP

There are five wall specimens (listed in Table 1) tested in this study. All specimens are 203cm in height , 240cm in width , and 1B in thickness. The mortar used in specimens is lime-cement mortar that used to simulate the URM wall built in the early 20th century. The volume ratio of lime to cement to sand is 1 : 1 : 3. For all specimens , the total opening area is the same , and the height of the opening is 70cm and the total width is 100cm. As shown in Fig.1 , for improving the stiffness at vertical edge of the wall and simulate the confined effect of connecting wall , the thickness at the vertical edge increases to 2B and plant six #5 reinforcing rebars. Besides , for transmit the lateral loading from the actuator to the specimen, a RC beam is arranged on the upper edge of the wall.

In the five specimens , W1 , W2 and W3 were tested under monotonic horizontal loading , and the influence of the disposition of the opening were to be discussed. The vertical load applying to these three specimens is 0.190kgf/cm^2 . W4 and W5 were tested under cyclic horizontal loading. The opening type of W4 and W5 are the same as W1. The vertical load of W4 is 0.190kgf/cm^2 , and for W5 is 0.725kgf/cm^2 which simulates the dead load transmitted from upper floor.

Table 1. Test Specimens

	Opening type	Loading type	Vertical load (kgf/cm ²)
W1	Uni-opening	Pushover load	0.191
W2	Two-opening	Pushover load	0.191
W3	Three-opening	Pushover load	0.191
W4	Uni-opening	Cyclic load	0.191
W5	Uni-opening	Cyclic load	0.725

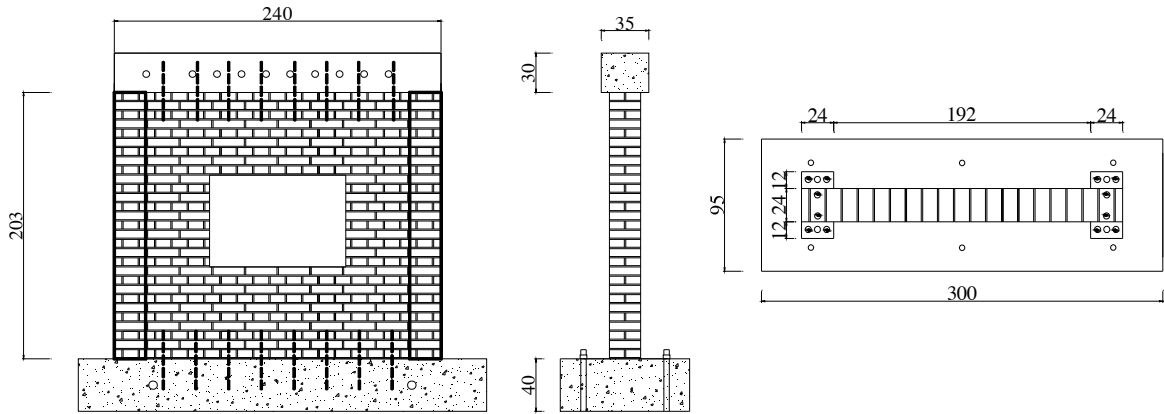


Figure 1. The specimen with one opening(W1,W4,W5)

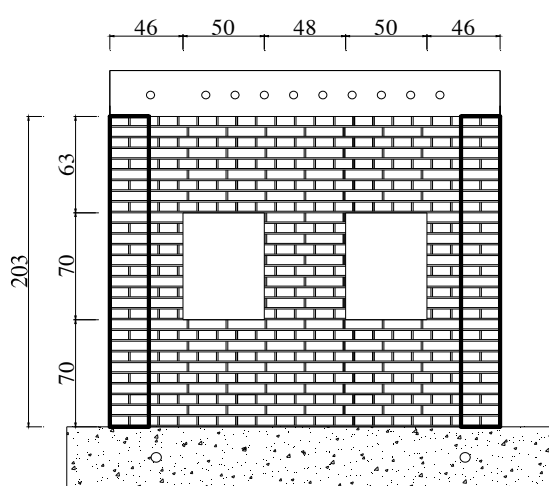


Figure 2. The specimen with two openings(W2)

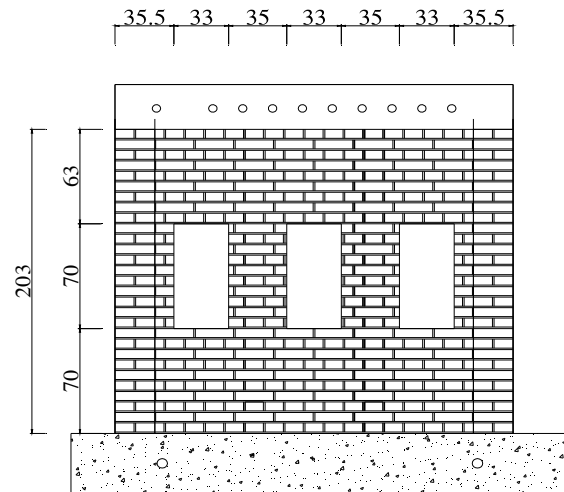


Figure 3. The specimen with three openings(W3)

2.2 Test Frame and Load Type

Fig. 4 is the test frame designed for this study. In the figure, the lower RC beam is fixed on the steel base by several high strength bolts. The upper RC beam and the steel cap are bolted together with 10 bolts (D=40mm). The end of the steel cap is connected to the actuator which is attached to the reaction wall. During test, the upper beam transmit the horizontal load to the top plane of the brick wall. Fig.5 is the vertical loading system which is assembled with lever and pulley system on top of the steel cap.

During test, applying loads are controlled by the stroke of the actuator. The stroke increased horizontal displacement 1mm per second. For cyclic loading, the stroke was controlled to increase 1mm cycle by cycle. The test is stopped as the specimen has been seriously damaged.

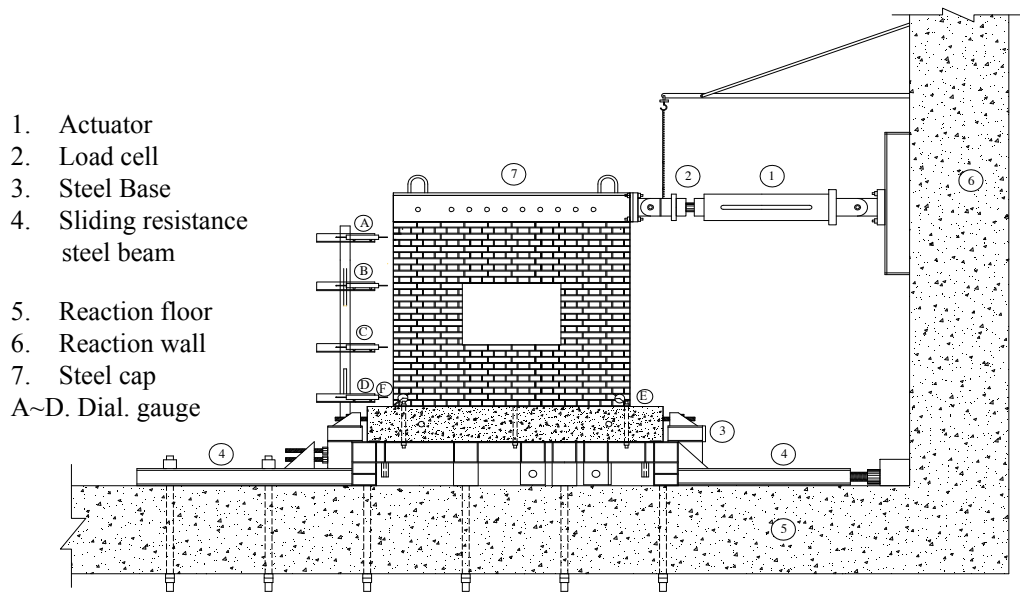


Figure 4. Test frame

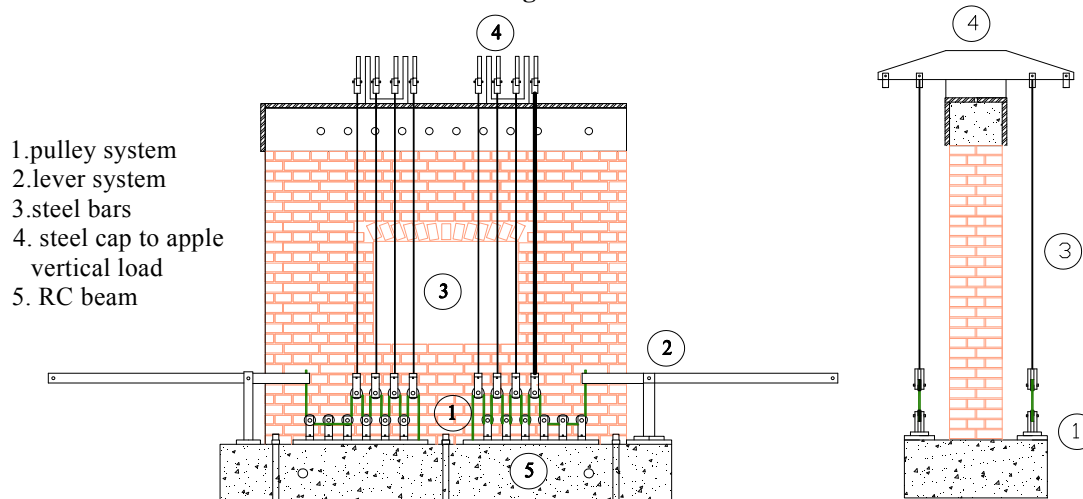


Figure 5. The additional vertical load applying system

3. TEST RESULTS AND DISCUSSION

3.1 The Material Properties

Table 2 lists the material properties of the specimens. For the traditional lime mortar in Taiwan, the lime needs to be put into the water more than one month for completely hydraulic reaction. However, the differences of material property still not be avoided for each specimen.

Table 2. The material properties

	Compressive strength of the brick (kgf/cm ²)	Compressive strength of the mortar (kgf/cm ²)	Shear strength of the joint (kgf/cm ²)	Tensile strength of the joint (kgf/cm ²)	Modulus of elasticity (kgf/cm ²)
W1	712.5	92.1	3.10	1.767	36145 28883 39680 37110
W2	712.5	115.9	3.08	2.194	
W3	712.5	100.4	3.07	1.682	
W4	712.5	97.16	3.78	1.935	
W5	712.5	130.0	fail	3.45	

3.2. The Behaviour of The Walls Tested Under Monotonic Loading(W1, W2 ,W3)

Fig.6 to Fig.8 were the damage mode of specimen W1 , W2 and W3 respectively. From the test , it is observed that the main damage modes of the wall with opening including the oblique shear cracks in the diagonal corner area and the horizontal cracks on the top and bottom of the piers between two openings. The horizontal cracks are caused by the combination of shear and bending stress. In general , the cracks extend almost along the interface between brick and mortar. This is due to the strength of the lime-cement mortar used in this study was much lower than the strength of the brick (Chen,2011). Further comparison of the oblique shear crack in the diagonal corner area , it could be found that the crack of W1 developed from the corner of the opening to the corner of the wall , but W2 and W3 did not. The width between edge of the opening and edge of the wall does affect the development of the crack path.

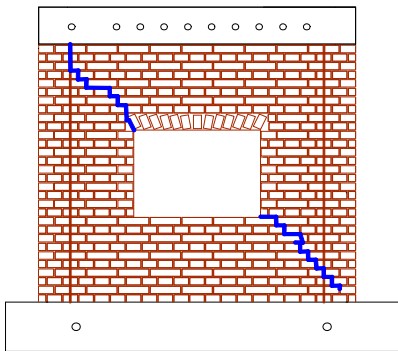


Figure 6. The damage mode of W1

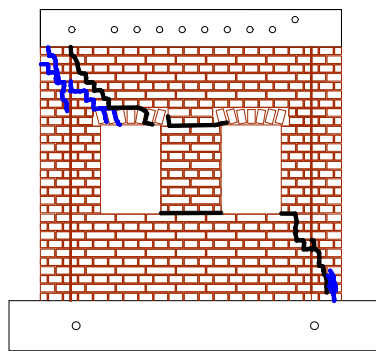


Figure 7. The damage mode of W2

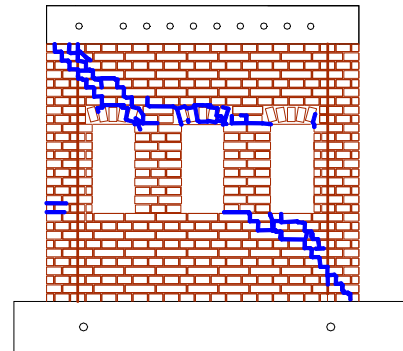


Figure 8. The damage mode of W3

Fig.9 gives the Load-Relative Drift angle relation of W1 , W2 and W3. The initial stiffness of these three walls did not appear much difference. However specimen W3 with three openings , decreased earlier than W1 and W2. The ultimate load of W3 is also the lowest.

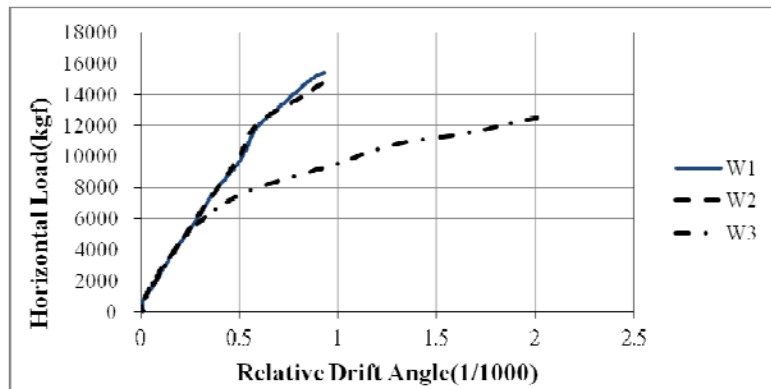


Figure 9. The comparison of W1,W2,W3

3.3. The Wall Behaviour Under In-Plane Cyclic Loading(W4 and W5)

Fig.10 and Fig.11 give the main damage modes of specimen W4 and W5 , respectively , tested under cyclic horizontal loading. In W4 , the cracks happened in sequence as the number shown in Fig.10. The wall in the diagonal corner area damaged first , and then the pier beside the opening also occurred crack. The associated slight cracks could be found in the area just aside main cracks. In W5 , subjected higher vertical load , all the cracks occurred almost at the same time. The damage mode is similar to that observed in W1(Fig.11). Also , in W5 as crack occurred , it is observed that the resistant capacity decreased immediately. Brittle damage mode is obvious for this specimen. Besides , it could also be found that some bricks were crushed in W5. This behavior will be more complicate in repair and conservation after earthquake.

The Load-Relative Drift angle relation of the W4 and W5 are shown in Fig.12 and Fig.13. The initial stiffness of these two specimens are approximate the same . However , as drift angle increasing , the

stiffness of W4 decreases earlier than W5. Specifically , for W4 , the diagonal corner area cracked under the load up to 18ton and the drift angle was 0.0036 , while W5 , the ultimate resistant load is 23ton and the corresponding drift angle was 0.00517. This result indicates that the wall subjected to high vertical load will be stiffer and have higher resistant strength , but the allowable drift angle will be lower.

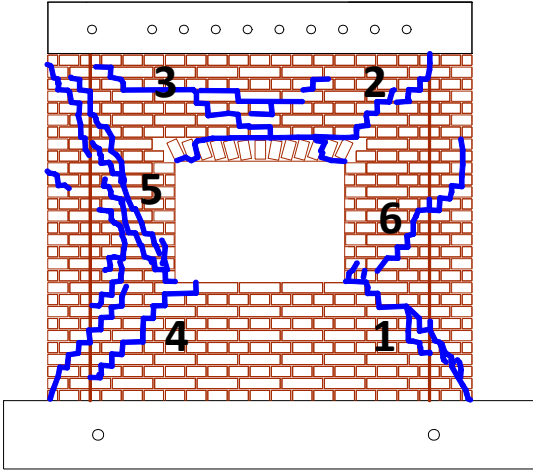


Figure 10. The damage mode of W4

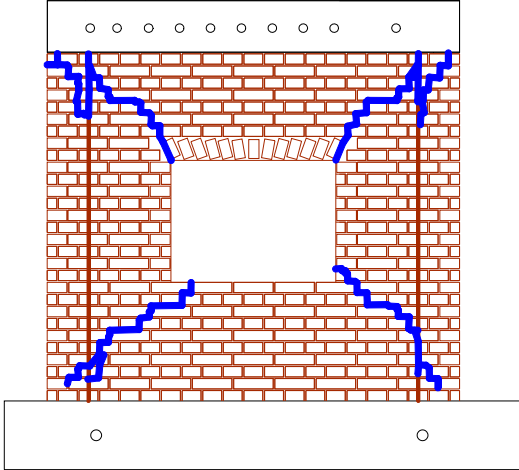


Figure 11. The damage mode of W5

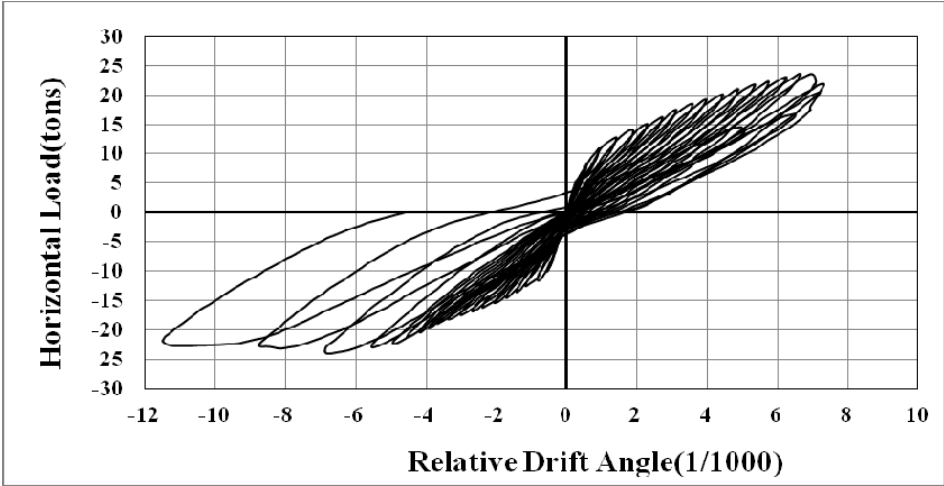


Figure 12. The load-drift angle relative curve of W4

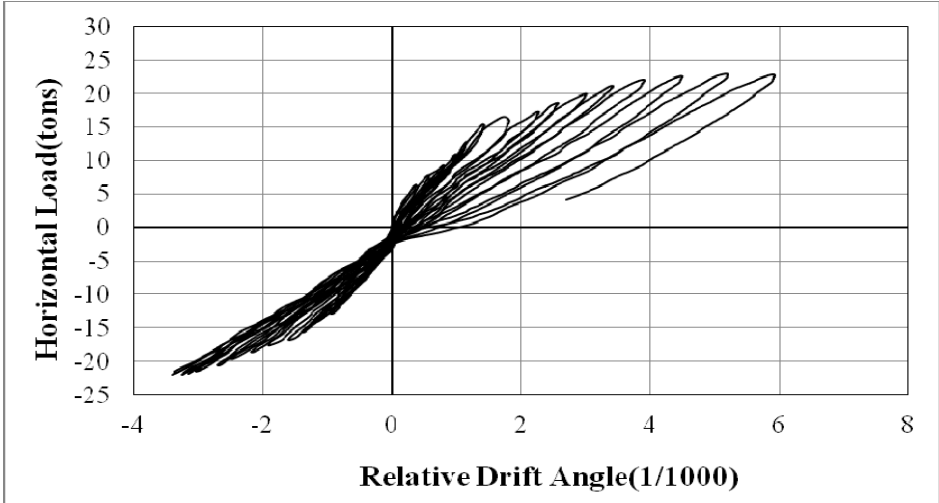


Figure 13. The load-drift angle relative curve of W5

4. EVALUATION OF ULTIMATE LOAD FOR THE WALL WITH OPENING

Based on the behavior observed in the test , following assumptions are adopted for the evaluation of the ultimate load :

- (1) Because the brick wall is the brittle material , all cracks damage simultaneously when the wall reaches the ultimate resistance strength.
- (2) For the diagonal corner area , the cracks are caused by the shear stress , and the contributing strength is symbolized by P_S .
- (3) For the pier , it is damaged by both shear stress and bending moment , and the contributing strength is symbolized by P_M .
- (4) The ultimate strength of the wall P_U is the sum of the strength ΣP_S plus the sum of the strength ΣP_M .

$$P_U = \Sigma P_S + \Sigma P_M \quad (4.1)$$

4.1. Calculation of P_S

For the ultimate strength of the URM wall occurred oblique shear cracks under in-plane loading , the calculation procedure has been developed by modelling the wall as a compressive truss (Chen,2009). The strength of the compressive truss depends on the shear strength of the joint . As shown in the Fig.14 , the stress of the wall element can be calculated by the stress of the compressive truss. According to the Mohr–Coulomb failure theory , the failure strength of the interface between the brick and mortar involves the shear stress τ_{xy} and the outward normal stress σ_{y0} , thus the ultimate strength of the compressive truss can be calculated by Eqn.4.2. However , the principal tensile strain of the wall element will cause the strength of the compressive truss decreasing. After considering the softening of principal compressive stress due to the principal tensile strain , the ultimate strength can be expressed by Eqn.4.5.

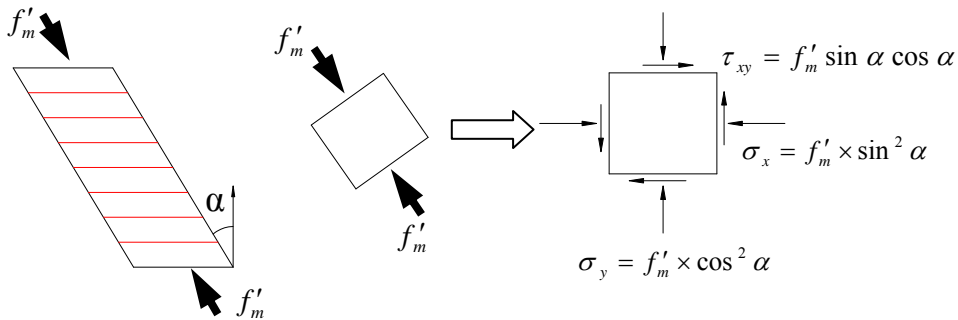


Figure 14. The relationship between the compressive truss and the wall element

$$f'_m = \frac{\tau_0 + 0.4 \times \sigma_{y0}}{\sin \alpha \cos \alpha - 0.4 \times \cos^2 \alpha} \quad (4.2)$$

$$\lambda = \beta \times \sin \alpha \quad (4.3)$$

$$\beta = -0.3998 \left(\frac{\sigma_{y0}}{f'_m} \right)^2 - 0.1248 \left(\frac{\sigma_{y0}}{f'_m} \right) + 1 \quad (4.4)$$

$$P_S = (\lambda \times f'_m \times \sin \alpha \cos \alpha) \times B_m \times T_m \quad (4.5)$$

τ_0 : Shear strength of interface between brick and mortar

λ : the soften ratio due to the principal tensile strain

α : the included angle between the crack and vertical axis

B_m :the width of the wall

T_m :the thickness of the wall

σ_{y0} :the stress caused by the vertical loading

4.2. Calculation of P_M

The damage mode of the pier indicates that it was confined by the wall upper and lower the opening. The horizontal crack of the pier was controlled by the moment of the end. Therefore, both end of the pier is assumed to a fix joint, and the pier damages when the tensile stress caused by the moment exceeds the allowable tensile strength of the wall. For the allowable tension strength σ_{yall} , it involves the outward normal stress σ_{y0} and the tension strength σ_t of the interface between brick and mortar.

$$\sigma_{yall} + \sigma_{y0} = \sigma_t \quad (4.6)$$

If the displacement on the top of the wall is Δ , the maximum normal stress caused by the moment can be written as Equ.4.7.

$$|\sigma_{MT}| = |\sigma_{MC}| = \frac{3E \times W \times \Delta}{H^2} \quad (4.7)$$

In the Eqn.4.7, σ_{MT} is the maximum tensile stress and σ_{MC} is the maximum compressive stress. Comparing σ_{MT} with σ_t , the strength P_{Cm} of the initial crack can be obtained:

$$P_{Cm} = \frac{T \times W^2 \times H \times (\sigma_t - \sigma_{y0})}{3} \quad (4.8)$$

4.2.1 The relationship between the displacement Δ and the width D of the horizontal crack

As the stress distribution shown in Fig.15, the outward normal stress σ_{y0} will increase because of the decrease of the sustain area. Thus, under the vertical load F_{y0} , the outward normal stress σ_{y0} is

$$\sigma_{y0} = \frac{-F_{y0}}{(W - D)T} \quad (4.9)$$

Here, D is the width of the horizontal crack. Then, the tensile stress σ_d caused by the moment at the tipping point C of undamaged area can be written as

$$\sigma_d = \sigma_t - \sigma_{y0} \quad (4.10)$$

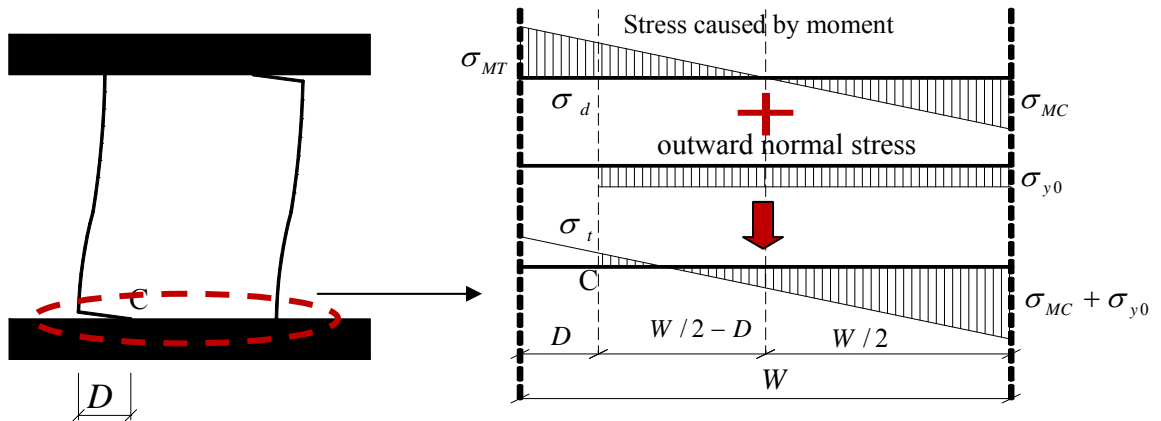


Figure 15. The stress distribution in the connection

For the stress caused by the moment, the relationship between stress σ_d and the ultimate stress σ_{MT} is

$$\frac{\sigma_d}{\sigma_{MT}} = \frac{W/2 - D}{W/2} \quad (4.11)$$

Replace Eqn.4.7 , Eqn.4.9 and Eqn.4.11 into Eqn.4.10 , we get

$$\frac{3E \times W \times \Delta}{H^2} \times \left(\frac{W}{2} - D\right) = \left(\sigma_i + \frac{F_{y0}}{(W-D)T}\right) \quad (4.12)$$

From Eqn.4.12 , we can calculate the width D of the crack , which is

$$D = \frac{\left(9W \times E \times T \times \Delta - H^2 \times T \times \sigma_i - \sqrt{(9W^2 \times E^2 \times T^2 + 6E \times H^2 \times T^2 \times W \times \sigma_i + 24F_{y0}H^2 \times E \times T) \times \Delta + H^4 \times T \times \sigma_i^2}\right)}{12E \times T \times \Delta} \quad (4.13)$$

Then , the acting moment M_D in the undamaged area can be obtained

$$M_D = \frac{3E \times I \times \Delta}{H^2} + \frac{2E \times T \times \Delta (W/2 - D)^2}{H^2} \quad (4.14)$$

4.2.2 The moment M_d caused by the vertical load

As shown in Fig.16 , when the both end of the pier occurred horizontal cracks , the vertical load would act the extra moment to the pier because of the eccentricity of the load. If the width of crack on the top and bottom end are D_T and D_B , assuming the vertical load locating at the centroid of the stress distribution where the resultant F_{y0} acts , the eccentricity can be calculated as

$$L_d = X_B - X_T = \frac{D_T + D_B}{2} - \Delta \quad (4.15)$$

Then , we can get the moment M_d caused by eccentricity of the vertical load

$$M_d = F_{y0} \times L_d = F_{y0} \left(\frac{D_T + D_B}{2} - \Delta\right) \quad (4.16)$$

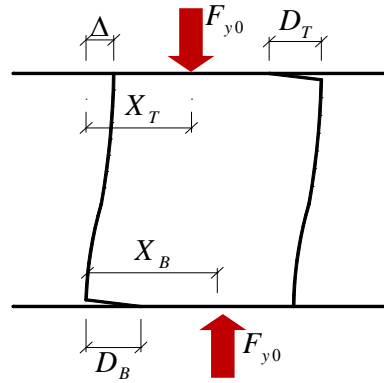


Figure 16. The eccentricity effect of the vertical load

4.2.3 The ultimate strength P_M

After obtaining the acting moment on the top and bottom end of the pier and the the eccentricity moment , the in-plane load V_M can be calculated by equating the moment of the pier.

$$V_M = \frac{M_{DT} + M_{DB} + M_d}{H} \quad (4.17)$$

Here , M_{DT} and M_{DB} are the moment in the undamaged area on the top and bottom end of the pier. As discussing previously , the shear failure strength of the interface between the brick and mortar is related to the shear strength of the interface and friction caused by the outward normal stress. So the allowable shear strength on the end of the pier can be obtained as

$$V_{all} = (W - D) \times \tau_0 + F_{y0} \times \mu = (W - D) \times \tau_0 + F_{y0} \times 0.4 \quad (4.18)$$

The ultimate resistant capacity of the pier P_M determines on when the V_M is equal to the allowable strength V_{all} .

$$V_{all} = V_M \quad (4.19)$$

5. COMPARISON OF ANALYTIC AND TEST RESULTS

The ultimate load of the wall specimens tested in this paper has been calculated using the procedure discussed previously and compared with test result. In Fig.17 , for the diagonal corner area , the included angle α between crack and vertical axis is 59° .

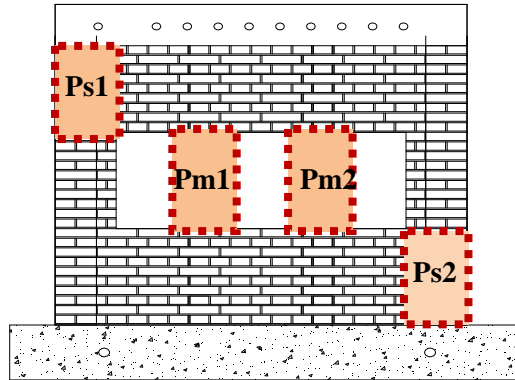


Figure 17. The strength assessing area of the wall

Table 3 lists the detail comparison of four wall specimens. In general , the calculation strength is close to the test result. Averagely , the difference is less than 4%. This result indicated that the seismic capacity of the wall with opening can be reasonably predicted. Further , comparing the contribution of Ps and Pm , the diagonal corner area is much greater than the pier . For wall specimen W2 and W3 which have multi-openings , the strength contribution of the pier is both less than 25%. Besides , it is observed that the strength contribution of the diagonal corner area Ps get decreased when the number of opening is increased. This is because the width between side opening and the wall vertical edge (the width of the Ps area) becomes smaller.

Table.3 The comparison between analysis and test result

	unit	W1	W2	W3	W4
Opening type		Uni-opening	Two-opening	Three-opening	Uni-opening
Diagonal corner area strength Ps1	kgf	7649	5637	4764	9296
Diagonal corner area strength Ps2	kgf	8003	5856	4924	9624
Pier strength Pm1	kgf		2297	1606	
Pier strength Pm2	kgf			1606	
Analysis ultimate strength P_u	kgf	15652	13790	12900	18910
Test strength T_u	kgf	15371	14731	12522	18510
Differential value $\frac{P_u - T_u}{T_u}$	%	1.83	-6.39	3.02	2.16
Strength contribution ratio of the Diagonal area $\Sigma Ps/P_u$	%	100	83.34	75.11	100
Strength contribution ratio of the pier $\Sigma Pm/P_u$	%		16.66	24.89	

6. CONCLUSIONS

In this paper , five brick wall specimens were manufactured with slime cement mortar to simulate the wall of historic building and tested under in-plane loading. The test result observed :

- (1) The main damage modes of the wall with opening included the oblique shear cracks in the diagonal corner area and the horizontal cracks on the top and bottom of the piers between two openings.

- (2) Because the strength of the mortar was much lower than the brick , the crack damaged along the interface between the brick and mortar.
- (3) For the diagonal corner area , the strength was visibly affected by the width between the side opening and the vertical edge of the wall.
- (4) Both of the strength of initial crack and ultimate strength of the wall diminished obviously when the number of the opening increased.

According to the failure mode observed from the experiment , a procedure for evaluating the ultimate strength of URM wall with opening is developed in this study. After comparing the evaluated ultimate strength with the ultimate load of four walls , the average difference is less than 4%.

REFERENCES

- Balasubramanian, S. R., K. B. Rao, D. Basu, M. B. Anoop, C. V. Vaidyanathan (2011). An Improved Method for Estimation of Elastic Lateral Stiffness of Brick Masonry Shear Walls with Openings. *Journal of Civil Engineering*. **15:2**, 281-293.
- Calderini C., S. Cattari and S. Lagomarsi (2009). In-plane strength of unreinforced masonry piers. *Earthquake Engineering and Structural Dynamics*.**38**, 243-267
- Chen, S.Y., F.L. Moon, T. Yi(2008). A macroelement for the nonlinear analysis of in-plane unreinforced masonry piers. *Engineering Structures*. **30**,2242–2252.
- Chen T.N. , Chang J.S. (2011). Experimental Investigation and Strength Evaluation of URM Wall with Slime mortar under In-Plane Loading. *Journal of Arthitecture*.**78**,39-61
- Chen T.N. , Chang J.S. (2009). Displacement of Masonry Wall Under Horizontal In-Plane Loading and It's Seismic Assessment Application, *Journal of Arthitecture*.**68,Special Issue on Technology**,15-24.
- Foraboschi P. (2009).Coupling effect between masonry spandrels and piers. *Materials and Structures* .**42**, 279-300
- Formica G. , V. Sansalone and R. Casciaro(2002). A mixed solution strategy for the nonlinear analysis of brick masonry walls. *Computer Methods in Applied Mechanics and Engineering*. **191**,5847-5876.
- Gideon P. A. G. van Zijl(2004).Modeling Masonry Shear-Compression: Role of Dilatancy Highlighted. *Journal of Engineering Mechanics*. **130:11**, 1289-1296.
- Rai D. C. and S. C. Goel (2007).Seismic Strengthening of Rocking-Critical Masonry Piers. *Journal of Structural Engineering*. **133:10**, 1445-1452
- Vermeltoort, A.Th, Raijmakers, Th.M.J, Janssen, H.J.M(1993).Shear tests on masonry walls. *Proceeding of the 6th North American masonry conference*.1183–1193.